Properties of Polystyrene/Organically Modified Layered Double Hydroxide Nanocomposites Synthesized by Solvent Blending Method

Balakrushna Sahu, G. Pugazhenthi

Department of Chemical Engineering, Indian Institute of Technology Guwahati, Guwahati 781039, India

Received 28 February 2010; accepted 27 September 2010
DOI 10.1002/app.33467
Published online 10 December 2010 in Wiley Online Library (wileyonlinelibrary.com).

ABSTRACT: In this work, organically modified layered double hydroxides (OLDHs) were prepared and used to make exfoliated polystyrene (PS) nanocomposites by solvent blending method. First, Mg-Al, Co-Al, Ni-Al, Cu-Al, Cu-Fe, and Cu-Cr LDHs were synthesized by coprecipitation method at constant pH using their nitrate salts. The organically modified LDHs (OLDHs) were synthesized using sodium dodecyl sulfate (SDS). Then, PS nanocomposites containing 5 wt % of the above modified LDHs were developed by solvent blending method. The structural and thermal properties of LDHs and their corresponding nanocomposites were characterized by X-ray diffraction (XRD), scanning electron microscopy (SEM), transmission electron microscopy (TEM), FTIR spectroscopy, and thermogravimetric analysis (TGA). The formation of exfoliated PS/OLDH nanocomposites is demonstrated by XRD and TEM analysis. TEM analysis also confirms the nanoscale dispersion of the LDH layers in the PS matrix. The presence of sulfate groups in the modified LDHs is confirmed by FTIR spectroscopy. The entire PS/OLDH nanocomposites exhibit enhanced thermal stability relative to pure PS. When 50% weight loss is selected as point of comparison, the decomposition temperature of the nanocomposites is about 5–13°C higher than that of pure PS. Water uptake of the PS nanocomposites is found to be less when compared to pure PS. © 2010 Wiley Periodicals, Inc. J Appl Polym Sci 120: 2485–2495, 2011

Key words: polystyrene; nanocomposites; thermal stability; XRD

INTRODUCTION

Development of the polymer nanocomposites is one of the latest evolutionary steps of the polymer technology due to dramatically improved properties such as mechanical and thermal properties,[1–4] gas permeability,[5,6] and fire retardance[7] compared with conventional composites. These enhanced properties are realized only when clay particles are well dispersed in the polymer matrix. Two types of nanocomposite structures can be obtained when the nanoparticles are dispersed in a polymer matrix. The intercalated nanocomposites are formed when there is a limited inclusion of polymer chain between the clay layers with a corresponding small increase in the interlayer spacing of a few nanometers. On the other hand, exfoliated structures are formed when the clay layers are well separated from each other and individually dispersed in the continuous polymer matrix. Many researchers have reported that the dispersion, or nanostructure, of the clay in the polymer determines the properties of that polymer-clay nanocomposite.[8–11] However, it is not known what level of clay dispersion (exfoliated or intercalated) is necessary for a particular property of interest.[8] It is generally assumed that exfoliation of the clay is preferred for the greatest increases in nanocomposite properties, but that may not always be correct. For example, it appears that in certain systems exfoliation is desired for mechanical properties, but not necessarily for flammability properties.[9–11]

There are four known ways to prepare polymer nanocomposites based upon the literature.[2,12–28] These include melt compounding,[12–15] *in situ* polymerization,[2,16–21] emulsion/suspension polymerization,[22,23] and solvent blending.[24–28] Among these methods, solvent blending has been a widely used technique, and it is one of the approaches that consistently give exfoliated materials, provided the clay organic treatment, solvent, and blending conditions are considered.[24–28]

Several attempts to prepare polystyrene-clay composites have been reported.[29–36] Friedlander and Grink[29] reported a slight expansion of the 001 spacing of clay galleries by *in situ* polymerization and concluded that polystyrene was intercalated in clay galleries; but Blumstein[30] questioned intercalation by polystyrene because he did not get any increase in the basal spacing. Later, Kato et al.[31] reported the

Correspondence to: G. Pugazhenthi (pugal@iitg.ernet.in).

intercalation of styrene into stearyl trimethyl-ammonium cation exchanged MMT. Kelly et al.[32] and Akelah et al.[33] reported the modification of MMT by a variety of functional groups while making epoxy composites. Akelah and Moet[34,35] have also prepared polystyrene nanocomposites using acetonitrile as a solvent. They reported the intercalation in PS-clay nanocomposites, with a maximum basal spacing of 2.54 nm. Vaia et al.[36] prepared intercalated polystyrene-clay nanocomposites by melt-intercalation method. Doh and Cho[37] prepared polystyrene-clay intercalated nanocomposites by polymerization of styrene in the presence of organophilic clay. The intercalated polystyrene-clay nanocomposites exhibited thermal stability better than pure polystyrene. Sohn et al.[38] prepared polymer nanocomposites based on an organophilically modified montmorillonite (OMMT) and polystyrene (PS) by solvent blending method using chloroform as a co solvent. Formation of intercalation nanocomposites was confirmed from the increase in interlayer spacing. The reactive cationic surfactant, vinyl benzyl dimethyl dodecyl ammonium chloride, VDAC was used for ion exchange with sodium ions in MMT. Then exfoliated polystyrene-clay nanocomposites were prepared by direct dispersion of organophilic MMT in styrene monomer followed by free radical polymerization.[39] Uthirakumar et al.[40] prepared the exfoliated polystyrene (PS)/clay nanocomposites via *in situ* polymerization using a cationic radical initiator-intercalated montmorillonite hybrid. The exfoliated structure resulted mainly due to the anchored radical initiator inside the clay galleries. Zhang et al.[41] prepared styrenic polymer/clay nanocomposites by melt blending of the polymers with an oligomerically modified clay. Bhiwankar and Weiss[42] used quaternary ammonium salts of sulfonated polystyrene (SPS) as compatibilizers for melt intercalation of PS and pristine Na-MMT.

The majority of previous studies have been focused on the montmorillonite type of layered silicate compounds,[43] whereas the LDH systems have much less studied because of the strong interlayer electrostatic interactions, small gallery space, and hydrophilic property of LDH. However, the highly tunable properties of LDHs are considered as a new emerging class of the most favorable layered crystals for preparation of multifunctional polymer/layered crystal nanocomposites.[44] LDHs are the materials consisting of positively charged metal oxide/hydroxide sheets with intercalated anions and water molecules.[45,46] The intercalated anions can be exchanged with wide variety of anionic species both of organic and inorganic, indicating that there is a wide field of potential applications of LDH materials.[47–52] One of the major advantages of LDHs is that, they can be synthesized in a laboratory with high purity and tunable chemical compositions.

Recently, a series of polymeric anions and water soluble polymers, such as poly(acrylate),[53] poly(amino acid),[54] poly(styrene sulfonate),[55] poly(vinyl sulfonate),[56] poly(ethylene oxide),[57] poly(vinyl alcohol),[58,59] and polyaniline[60] have been used for preparing intercalated polymer/LDHs nanocomposites by ion-exchange reaction or *in situ* polymerization. However, the above methods are very difficult to use for the preparation of exfoliated polymer/LDH nanocomposites except for the organo-modified LDH layers. O'Leary and coworkers[43] have reported that the delamination of the dodecyl sulfate-modified Mg/Al LDH in polar acrylate monomers, with the help of high shearing and subsequent polymerization of the monomers containing the LDH dispersion gave exfoliated polyacrylate/LDH nanocomposites. Hsueh and Chen[61,62] have obtained polyimide/LDH and epoxy/LDH nanocomposites from the amino benzoate-intercalated and amino laurate-intercalated Mg-Al LDH, respectively.

In this work, we made an attempt to prepare polystyrene nanocomposites using organically modified Mg-Al, Co-Al, Ni-Al, Cu-Al, Cu-Fe, and Cu-Cr LDHs by solvent blending method and investigated their structural and thermal properties.

EXPERIMENTAL

For the synthesis of polymer nanocomposites, pristine LDH is not suitable because of its very small interlayer spacing which makes the insertion of polymeric chains very difficult. Hence pretreatment of LDHs are necessary. This pretreatment involves the insertion of organic anionic species having a long hydrophobic tail. This causes expansion of the interlayer distance and also it makes LDHs more compatible with organic polymers. There are mainly three methods for modification of LDHs, reported in literature such as: coprecipitation in the presence of organic species, ion exchange method, and regeneration method. The regeneration method is most advantageous because, competing anions (NO_3^-) is absent or minimum in this case. Most of the LDH clays can regenerate their original structures from their oxide form when they are dispersed in an aqueous solution containing the anion present in the original material. Six different combinations of LDH such as Mg-Al, Co-Al, Ni-Al, Cu-Al, Cu-Fe, and Cu-Cr are prepared by coprecipitation method. The LDHs are modified by sodium dodecyl sulfate ($NaC_{12}H_{25}SO_4$) using regeneration method and PS/OLDH nanocomposites are prepared using these modified LDHs by solvent blending method.

Materials

Mg $(NO_3)_2.6H_2O$, Cu $(NO_3)_2.3H_2O$, Ni $(NO_3)_2.6H_2O$, Co $(NO_3)_2.6H_2O$, Al $(NO_3)_3.9H_2O$, $Cr(NO_3)_3.9H_2O$, $Fe(NO_3)_3.9H_2O$, $NaNO_3$, NaOH, xylene, and sodium dodecyl sulfate (SDS) ($NaC_{12}H_{25}SO_4$) were purchased from Merck, India. Polystyrene was procured from National Chemicals, India. All the chemicals were used as received without further purification. Millipore water was used throughout this work.

Preparation of LDHs

All the LDHs (Mg-Al, Co-Al, Ni-Al, Cu-Al, Cu-Fe, and Cu-Cr) were prepared by coprecipitation method. First, an aqueous solution of nitrate of a bivalent metal (Mg/Co/Ni/Cu) (0.12 mol), Al $(NO_3)_3.9H_2O$, (0.06 mol) and $NaNO_3$ (0.12 mol) were prepared. A M^{2+}/M^{3+} ratio of 2 : 1 was maintained for all LDHs synthesis. To this, an aqueous solution of NaOH (2*M*) was added drop wise with vigorous stirring until the required pH is obtained. A pH of 10, 8.3, 10, 10.7, 9, and 10.2 were maintained for Mg-Al, Co-Al, Ni-Al, Cu-Al, Cu-Fe, and Cu-Cr LDHs, respectively.[5,6] The resulting slurry was aged at room temperature for 16 h. Then the resultant precipitate was filtered, washed thoroughly with Millipore water until the pH of the filtrate was neutral, and subsequently dried at 80°C for 12 h.

LDH modification

All the LDHs were modified with SDS for better dispersion of LDH materials in the polymer matrix. First, the LDH samples (2.5 g) were calcined at 500°C for 5 h in a muffle furnace (air atmosphere) with a heating rate of 2°C min^{-1} to obtain the oxide form. Then the calcined LDHs were dispersed into a 120 mL of aqueous solution containing 2.5 g of SDS. This dispersion was refluxed for 12 h to ensure complete regeneration of the host LDH structure. Finally the residues were separated by centrifuging and washed with Millipore water several times to get rid of unreacted surfactant molecules. The solids were dried at 80°C to produce organically modified LDHs.

Preparation of polystyrene/LDH nanocomposites

The OLDH loading was kept constant at 5 wt % (relative to PS) for all the PS/OLDH nanocomposite systems. PS/OLDH nanocomposites were prepared by solvent blending method in which xylene was used as a solvent. A known quantity of polystyrene was added to xylene with continuous stirring at room temperature until the PS was completely dissolved. After that, an organically modified LDH was added into the above polymer solution and ultrasonicated for better dispersion of LDH material in the polymer matrix. Then it was spread over a glass plate and left for 12 h in ambient temperature yielding a viscous gel layer. Finally the film was heated in an oven for 6 h to remove the remaining solvent to obtain PS/OLDH nanocomposites. The prepared nanocomposite films were characterized for structural and thermal properties. The pure PS film was also prepared by an identical procedure in the absence of LDH.

Characterization and measurement

X-ray diffraction (XRD) profile of different LDHs and nanocomposites samples were recorded under air at room temperature using AXS D8 ADVANCE Fully Automatic Powder X-ray Diffractometer (Bruker). The patterns were acquired for 2θ range of 2°–50° with a 0.05° s^{-1} scan speed. XRD pattern was used to interpret with respect to the position of the basal peak, which depends on the distance between two adjacent metal hydroxide sheets in the LDH crystal lattice. The morphology of LDHs powder was analyzed on a variable Pressure Digital Scanning Electron Microscope (model LEO 1430VP). The transmission electron microscopy (TEM) image of the PS nanocomposite was obtained on a JEOL JEM-2100 transmission electron micro analyzer with an accelerating voltage of 200 KV. The synthesized LDHs were analyzed using Perkin–Elmer Fourier transform infrared spectroscope to confirm the presence of OH^- groups and sulfate bands in the modified LDH sample. The thermogravimetry (TG) analysis for thermal stability was performed under nitrogen atmosphere on a TGA/SDTA851e/LF/1100 model (Mettler Toledo) instrument using a heating rate of 10°C min^{-1} from 25 to 900°C. The particle size analyses of the synthesized LDH were done using Dynamic Light Scattering Particle Size Analyser LB-550 (Horriba). Millipore water was used as a dispersing medium in this process.

The water uptake test was considered as a standard method to evaluate water resistance of the nanocomposite films using gravimetric method. Water uptake of the nanocomposite films were determined by measuring the change in the weight before and after the hydration. Three samples of each nanocomposite films (having dimensions 3 cm × 3 cm) were dried at 100°C for 4 h to bring each sample to an identical starting state. The nanocomposite samples were then weighed to note the dry weight. Finally the dried samples were soaked in millipore water for 48 h. Then they were taken out, wiped with tissue paper and weighed immediately. The water

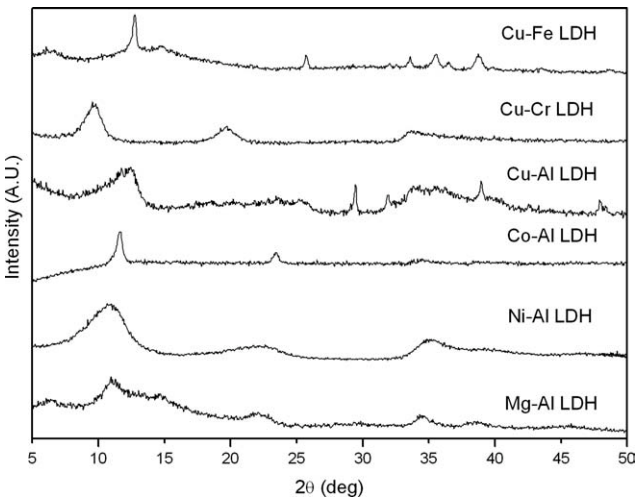

Figure 1 XRD patterns of pristine LDHs.

uptake of the nanocomposite films were calculated using Eq. (1)

$$\text{Water uptake (wt\%)} = \frac{W_w - W_d}{W_d} \times 100 \qquad (1)$$

where, W_w and W_d are the weights of wet and dry nanocomposite films, respectively.

RESULTS AND DISCUSSION

Characterization of LDHs

The XRD pattern of pristine LDHs and organically modified LDHs (OLDHs) in the 2θ range of 2°–50° is shown in Figures 1 and 2. The main diffraction peak of Mg-Al, Co-Al, Ni-Al, Cu-Al, Cu-Fe, Cu-Cr LDHs are obtained at 2θ values 11.16°, 11.57°, 11.4°, 12.35°, 12.75°, and 9.55°, respectively, that correspond to a (003) spacing of pristine LDHs. These peaks demonstrate the formation of LDHs and exhibit some common features of layered materials such as narrow, symmetric, strong peaks at low 2θ values and weaker, less symmetric lines at high 2θ values. The position of the basal peak of LDHs indicates the distance between two adjacent metal hydroxide sheets. The *d*-spacing value of Mg-Al, Co-Al, Ni-Al, Cu-Al, Cu-Fe, Cu-Cr LDHs is calculated as 0.790, 0.764, 0.762, 0.716, 0.69, and 0.926 nm by using Bragg's equation $d = \lambda/2\sin\theta$, where λ is the X-ray wavelength (1.5418 Å). This value is related to the thickness of the brucite like layers as well as the size of the anion and the number of the water molecules existing in the interlayer. With such small interlayer distance, it becomes necessary to modify the pristine materials so that the crystal layers are moved apart and penetration of polymeric chains becomes less difficult. The rehydration method for intercalating LDH materials with large molecules was pioneered in late 1980s. This method is based on the principle that the calcined LDH (which are mostly mixed metal oxides) regenerates the crystalline structure of the original materials when dispersed in an aqueous solution of suitable anion under ambient conditions. To eliminate the stronger electrostatic interactions between the LDH layers and obtain the intercalated or exfoliated structures, the surfactants are usually applied to modify the surface property of the LDH layers, which has been proven to be an effective method.[63,64] In this study, sodium dodecyl sulfate (SDS) is used to modify the pristine LDHs. When the LDHs are modified with SDS, the peak (003) is shifted slightly towards the left, correspondingly increasing the *d*-spacing, which confirms the intercalation of SDS molecules into the clay galleries[65] (see Fig. 2). The main diffraction peak of OMg-Al, OCo-Al, ONi-Al, OCu-Al, OCu-Fe, OCu-Cr LDHs is obtained at 2θ values of 3.2°, 4.75°, 5.3°, 4.50°, 4.15°, 7.45°, respectively. The d_{003} spacing of OMg-Al, OCo-Al, ONi-Al, OCu-Al, OCu-Fe, OCu-Cr LDHs is found to be 2.757, 1.858, 1.667, 1.961, 2.126, 1.185 nm, respectively. The increase in *d*-spacing of OLDHs indicates that the hydrophilic layer surface changes into organophilic. Thus the PS chains can be more easily intercalated into the space of the LDH layers. We were also calculated the crystalline size from the Scherrer equation:

$$D = \frac{k\lambda}{\beta \cos\theta} \qquad (2)$$

where k is a constant ~ 0.9, λ is the wavelength of the X-rays which is 0.15418 nm, β is the full width of diffraction peak at half maximum intensity, and θ is the Bragg angle. The calculated crystalline sizes of the modified LDHs (OLDHs) are found to be in the

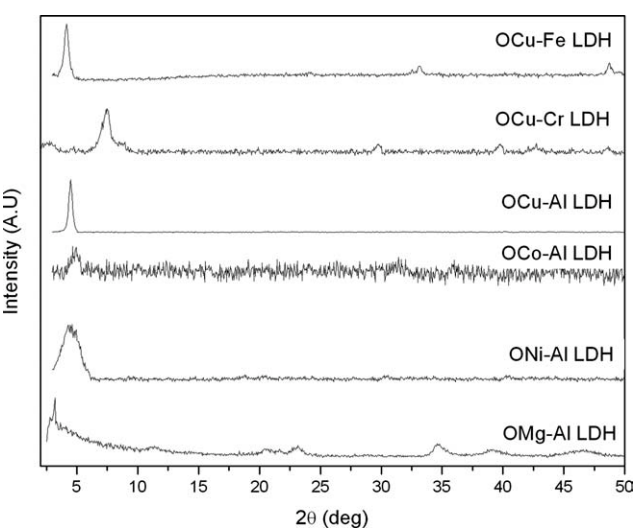

Figure 2 XRD patterns of organically modified LDHs.

TABLE I
Crystalline Size and *d*-Spacing of Pristine LDHs

Name of sample	2θ (deg.)	*d*-spacing (nm)	Crystal size (nm)	Matching JCPDS file no.
Cu-Al LDH	12.35	0.716	3.98	037-0630
Ni-Al LDH	11.4	0.762	2.48	022-0452
Co-Al LDH	11.57	0.764	15.98	051-0045
Mg-Al LDH	11.16	0.790	18.25	022-700
Cu-Fe LDH	12.75	0.690	20.74	–
Cu-Cr LDH	9.55	0.926	6.045	

range of 5–94 nm. The *d*-spacing and crystalline sizes of pristine and modified LDHs are listed in Tables I and II.

Figure 3 shows the SEM images of organically modified LDHs. It can be seen clearly that all LDHs are present in the form of agglomerates with having sizes of 1–7 μm. For Cu-Al LDH, some agglomerates are having sizes smaller than 1 μm. This observation suggests that the nanoparticles are generally in the form of agglomerates and it's rather hard to be dispersed in their initial dimensions. However, this can be eliminated by ultrasonication. The formation and modification of LDHs are confirmed from EDX analysis (figure is not shown here).

FTIR technique has been used to identify the nature and symmetry of interlayer anions. The FTIR spectra of the modified LDHs show two types of bands: one corresponding to the anionic species intercalated and the other corresponding to the host LDH materials. FTIR spectra of organically modified LDHs are similar as shown in Figure 4. The broad band in the range of 3400–3500 $cm^{-1}$is due to O—H stretching vibration of water molecules, which may be adsorbed during the sample preparation for FTIR. The stretching band for aliphatic CH_3— or —CH_2— of the long chain of SDS molecules appears at around 2840–2920 cm^{-1}. The small band between 1200 and 1220 cm^{-1} corresponds to the symmetric vibration ($\nu_{S=O}$) and the band between 1050 and 1100 cm^{-1} corresponds to the asymmetric vibration ($\nu_{oS=O}$) of sulfate band, which the LDHs acquired from SDS after modification. The bands recorded at low frequency region of 400–800 cm^{-1} are attributed to the vibration of metal-oxygen bond in the brucite like lattice and is typical of this kind of layered solids.

Generally, the thermal stability of LDH materials depends on many factors such as the nature of the cations, cationic compositions in the brucite-like layer, the nature of interlayer anions, the crystallinity of the materials, etc. The thermal behavior of LDHs has been studied in details before. Many researchers reported that the LDHs follow a two stage decomposition process: first, at low temperatures up to 225°C is assigned to the removal of water physisorbed on the external surface of the crystallites as well as water intercalated in the interlayer galleries; and the second at higher temperatures around 500–600°C is due to dehydroxylation of metal hydroxide layer along with simultaneous removal of anions. The thermal characteristics of the pristine LDHs are determined by TGA as shown in Figure 5(a). The weight losses for Cu-Cr, Cu-Al, and Ni-Al LDHs up to 250°C are 24, 23, and 18%, respectively, while the weight loss for Co-Al, Mg-Al, and Cu-Fe LDHs are up to same temperature are only 14, 15, and 16%, respectively. The reason for difference in the weight loss up to 250°C may be due to the different in layer charge density of the LDH material and the amount of the physically adsorbed water present in the LDH sample in addition to the water intercalated in the interlayer galleries. It is reported in the literature that higher layer charge density LDH material offers more combined hydroxyls, water molecules and nitrates.[66] The main weight loss occurs from 100 to 350°C that corresponds to the decomposition of anions and desorption of water produced from the dehydroxylation process. When 10% weight loss is taken as point of comparison, the decomposition temperature of Mg-Al, Cu-Fe, Cu-Cr, Cu-Al, Ni-Al, and Co-Al LDHs is found to be 164, 216, 138, 141, 133, and 230°C, respectively. The residues obtained at 900°C are estimated as 51, 76.2, 64, 57.2, 57.8, and 69.1% for Mg-Al, Cu-Fe, Cu-Cr, Cu-Al, Ni-Al, and Co-Al LDHs, respectively.

The TGA curves of organically modified LDHs are shown in Figure 5(b). After modification with SDS, the thermal behavior of the LDHs is changed significantly. The decomposition dodecylsulfate ions take place in the range of 210–250°C. The loss of

TABLE II
Crystalline Size and *d*-Spacing of Organically Modified LDHs

Name of sample	2θ (deg.)	*d*-spacing (nm)	Crystal size (nm)
OCu-Al LDH	4.5	1.961	24.081
ONi-Al LDH	5.3	1.667	5.031
OCo-Al LDH	4.75	1.858	7.949
OMg-Al LDH	3.20	2.757	72.253
OCu-Fe LDH	4.15	2.126	20.377
OCu-Cr LDH	7.45	1.185	93.657

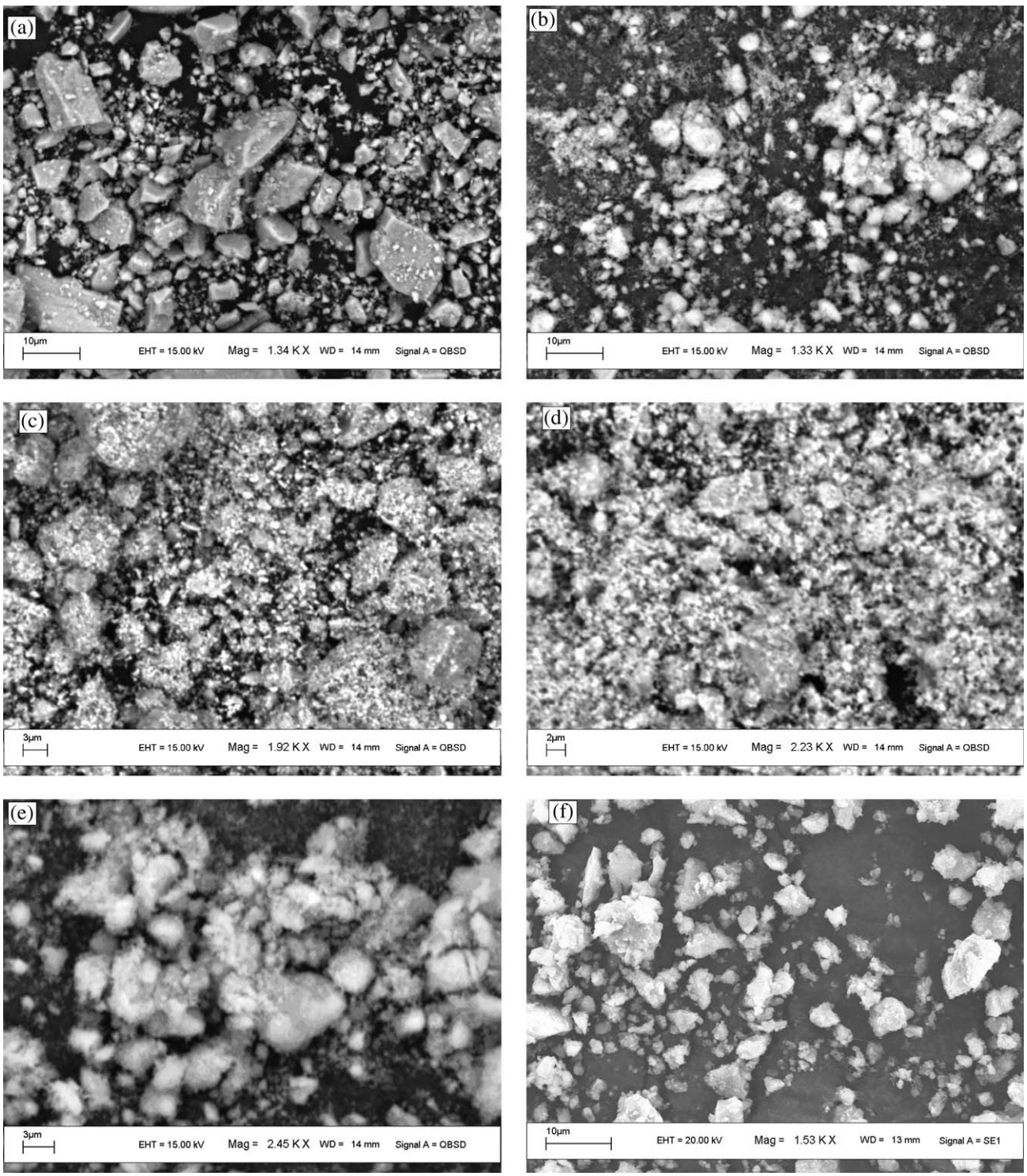

Figure 3 SEM images of (a) ONi-Al LDH, (b) OCu-Al LDH, (c) OCu-Fe LDH, (d) OCo-Al LDH, (e) OCu-Cr LDH, and (f) OMg-Al LDHs.

remaining nitrate ions and dehydroxylation of the host LDH layers take place at a slower rate at 250–350°C. However, the major dehydroxylation process of the OLDH materials starts around at 350°C. The weight losses for OCu-Al, ONi-Al, and OCo-Al LDHs up to 250°C are 7, 6, and 5%, respectively, while the weight losses for OCu-Cr and OCu-Fe LDHs up to same temperature are only 2.5 and 2.2%, respectively. The weight loss for OMg-Al LDH is 23%, which is highest among all LDHs. When 10% weight loss is taken as point of comparison, the decomposition temperature of OMg-Al, OCu-Cr, OCu-Al, ONi-Al, and OCo-Al LDHs is found to be 216, 797, 329, 430, and 545°C, respectively.

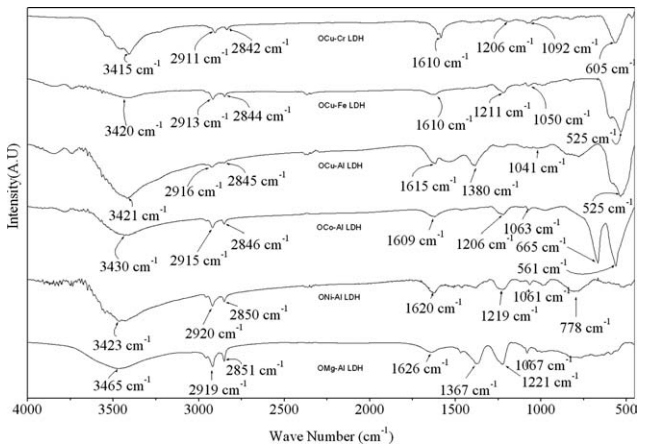

Figure 4 FTIR spectra of organically modified LDHs.

Maximum degradation in case of Cu-Fe LDH at 900°C is found to be 5.4%. The residues obtained at 900°C are 49.5, 94.6, 89.2, 88.2, 83.7, and 86.5% for OMg-Al, OCu-Fe, OCu-Cr, OCu-Al, ONi-Al, and OCo-Al LDHs, respectively.

From the DLS particle size analysis data (Fig. 6), it is pretty clear that the synthesized OLDHs have more than 85% particles below 500 nm. DLS results indicate that the particle sizes are bigger than those indicated by XRD. However, it is to be noted that DLS results are obtained in the liquid phase. Thus aggregation cannot be ruled out and the measurements may indeed be aggregated particles rather than the individual primary particles. It is observed that about 5% of the LDH particles are very close to nano range, i.e., close to 100 nm.

Characterization of PS/OLDH nanocomposites

XRD analysis

XRD is an effective tool to characterize the types of the layered structure, that is, intercalated and/or exfoliated polymer/LDH nanocomposites because the peaks changed with the gallery height of the LDH. In the case of intercalated nanocomposite, a XRD peak is seen at larger *d*-spacing than in the pristine LDH where as in case of exfoliated structure, no peak is seen. However the XRD patterns of PS/OLDH nanocomposites as shown in Figure 7 do not exhibit any peak (d_{003}) corresponding to the OLDH, which indicates that the organically modified LDH layers are exfoliated in the PS matrix.[67,68] These results demonstrate the successful formation of PS/OLDH nanocomposites via solvent blending. The nanocomposites demonstrate a slightly lower degree of crystallinity compared to the neat polystyrene. The presence of LDH layers restricts large crystalline domains from forming due to limited space and restrictions imposed on polymer chains by a large number of disordered LDH platelets, this leads to smaller crystallite structures and more defect-ridden crystalline lamella.

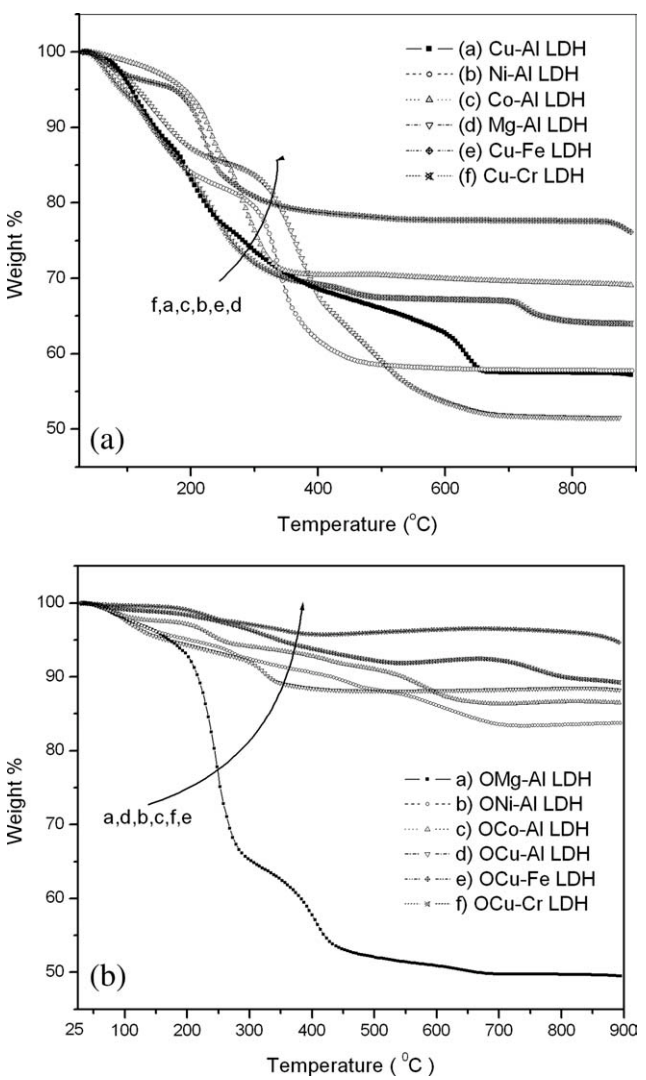

Figure 5 (a) TG analysis of pristine LDHs. (b) TG analysis of organically modified LDHs.

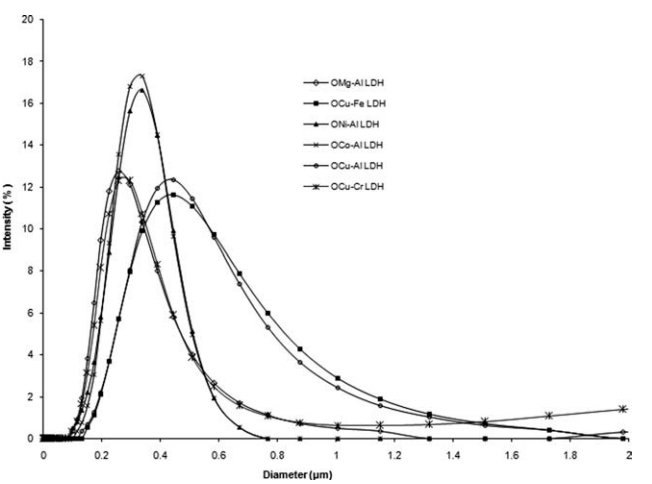

Figure 6 Particle size distribution of synthesized LDHs.

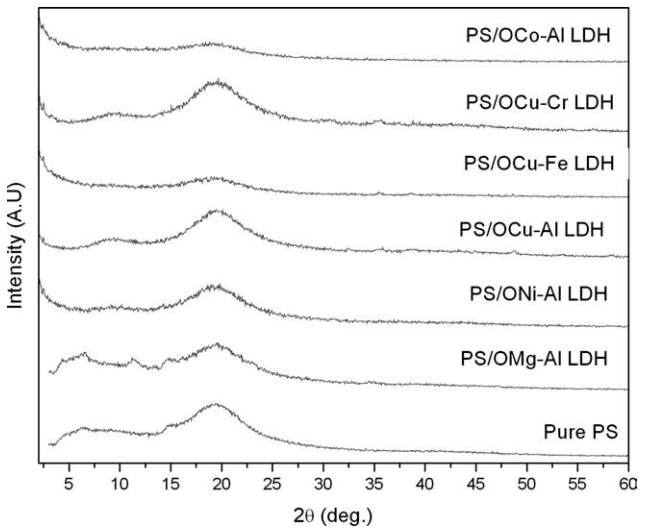

Figure 7 XRD patterns of PS/Organically modified LDH nanocomposites.

To study the influence of LDH loading on the structure of PS nanocomposite, we have prepared PS/OCo-Al LDH nanocomposites with 3, 5, and 20 wt % OCo-Al LDH content and their XRD results are depicted in Figure 8. It is observed that the basal spacing of OCo-Al LDH component in the nanocomposites increases to 2.76 nm from 1.86 nm of the original OLDH layers with decreasing content of OCo-Al LDH to 20 wt % from 100 wt % because of the intercalation of PS molecules into the LDH layers. When the loading of OCo-Al LDH is below 5 wt %, no diffraction peak is observed in 2θ range between 2° and 5°, as shown in Figure 8. These data demonstrate that the equilibrium between exfoliation and intercalation structures in the PS/OCo-Al LDH nanocomposites can be driven towards to exfoliation by decreasing the content of LDH. Finally, completely exfoliated PS/OCo-Al LDH nanocomposites can be obtained by decreasing the LDH content to below 5 wt %.

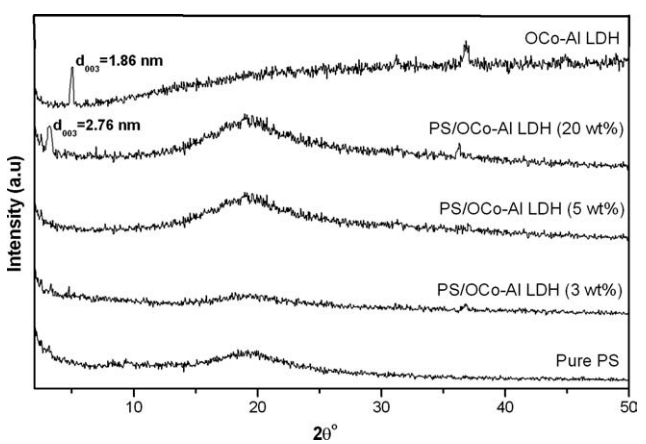

Figure 8 XRD patterns of OCo-Al LDH, pure PS and PS/OCo-Al LDH nanocomposites with various loading of OCo-Al LDH (3, 5, and 20 wt %) samples.

TEM study

The exfoliated structure of PS/OCo-Al LDH nanocomposite is further studied by TEM analysis. From TEM image (Fig. 9), the dark lines represent the LDH layers, whereas the bright areas represent PS matrix. The photograph clearly shows the lamellar structure of LDH exfoliated by the PS macromolecular chain; the lines of the layers are well shown using the arrow marks and the exfoliated OCo-Al LDH sheets are dispersed in the PS matrix, being consistent with the XRD results presented in Figure 8. The OCo-Al LDH platelets might be broken into smaller ones during ultrasonication.

Thermogravimetric analysis

Figure 10 represents the TGA curve of pure PS and PS/OLDH nanocomposites. The thermal decomposition of pure PS sample occurs in the range of 350–450°C. Generally, the PS/OLDH samples exhibit three different types of weight losses. The first step of weight loss at about 120–250°C is due to the evaporation of physically absorbed water in the interlayer and the loss of hydroxide on LDH layers. The second step of weight loss between 250 and 450°C is attributed to the thermal degradation of PS chains and formation of black charred residues. The degradation rate of PS nanocomposites in this step is much slower when compared to pure PS. It may be due to the hindrance of LDH layers to diffusion of

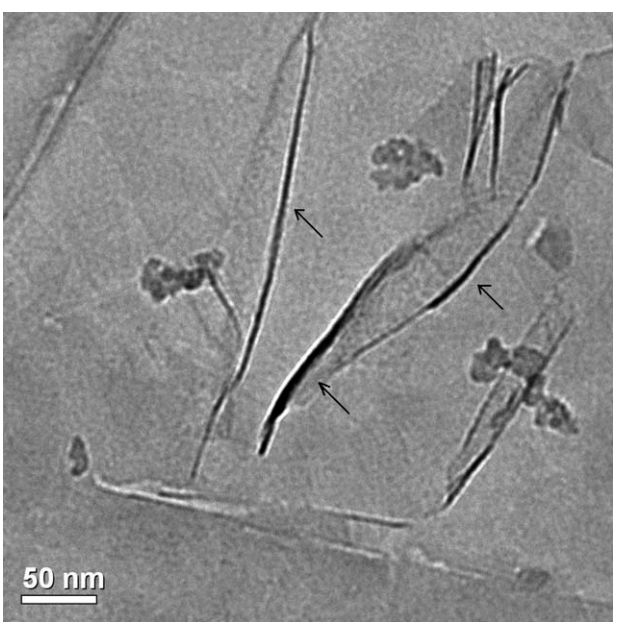

Figure 9 TEM image of PS/OCo-Al LDH nanocomposite with 5 wt % LDH.

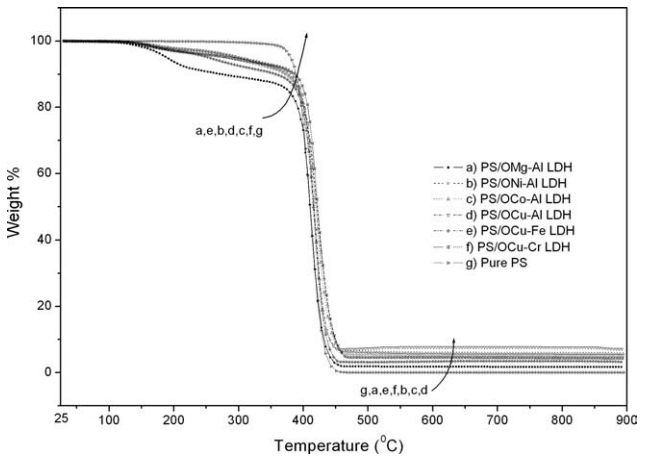

Figure 10 TG analysis of PS/OLDH nanocomposites between 25 and 900°C.

the volatile products produced during the heating of PS/OLDH nanocomposites. The final step is the decomposition of the charred residues which generally occur at around 650°C. When 10% weight is chosen as a point of comparison, the decomposition temperature are 387, 375, 370, 357, 385, 380, and 270°C for pure PS, PS/OCu-Al, PS/ONi-Al, PS/OCu-Fe, PS/OCu-Cr, PS/OCo-Al, and PS/OMg-Al LDH nanocomposites, respectively. It clearly demonstrates that the thermal decomposition temperature of nanocomposites is relatively lower than the pure PS. This is because of two reasons; LDHs can catalyze the degradation of PS and LDHs are dispersed disorderly in the PS matrix which is more efficient to catalyze the degradation of PS. However, the PS/OLDH nanocomposites show better thermal stability at high temperatures (above 400°C), which is confirmed by shifting the TGA curve of the PS/OLDH nanocomposites towards right of the TGA curve for pure PS (see Fig. 11). When 50 wt % is chosen as a point of reference, the decomposition temperature of

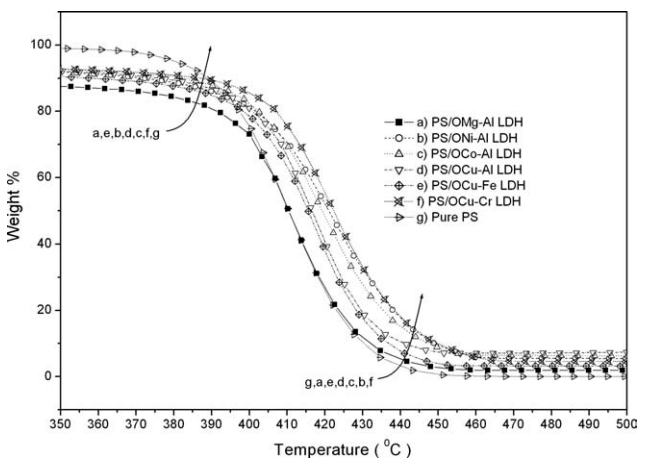

Figure 11 TG analysis of PS/OLDH nanocomposites between 350 and 500°C.

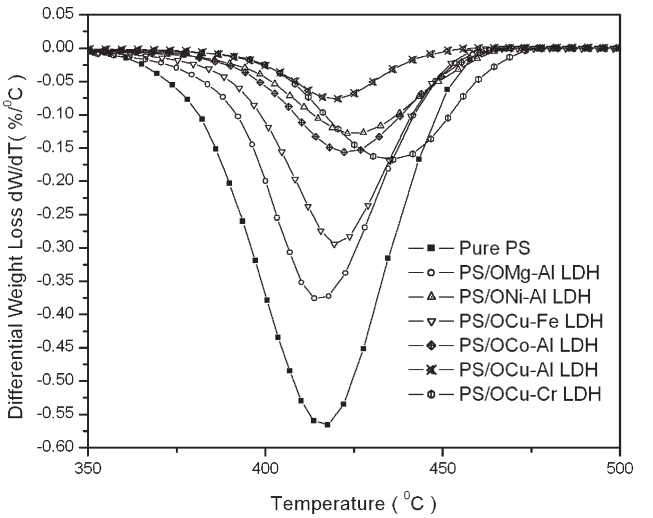

Figure 12 TGA derivative of PS/OLDH nanocomposites.

PS/OCu-Fe, PS/OCu-Al, PS/OCo-Al, PSONi-Al, and PS/OCu-Cr is found to be 415, 416, 419, 421, and 423°C, respectively. This implies that at 50 wt % loss, the PS/OLDH nanocomposites show a higher thermal stability of 5–13°C in comparison with pure PS. However, the decomposition temperature of PS/OMg-Al is found to be 410°C, which is almost same as pure PS. This may be due to the excess loading/or instability of surfactant as evidenced from the TGA data (see Fig. 5). Previous work has proved that the LDH sheets can provide polymer good thermal stability but too much LDH in the polymer matrix can cause polymer to decompose quickly.[69,70] The first TGA derivative curve for pure PS and PS/OLDH nanocomposites is shown in Figure 12. The peak indicates the maximum degradation temperature. All the first TGA derivative curves of PS/OLDH nanocomposites are shifted toward right side that of pure PS indicating higher thermal stability. Therefore, an improvement in the thermal stability will lead to the better service performance of the nanocomposites at an elevated temperature. Similar results have also been observed by other researchers.[40] The TGA results for pure PS and PS/OLDH nanocomposites are given in Table III.

TABLE III
TGA Results for Pure PS and PS/OLDH Nanocomposites

Name of sample	Temperature at 10% (wt) degradation in °C (T_{10})	Temperature at 50% (wt) degradation in °C (T_{50})	ΔT_{50} (°C)
Pure PS	387	410	–
PS/OMg-Al LDH	270	410	0
PS/OCo-Al LDH	380	419	9
PS/ONi-Al LDH	370	421	11
PS/OCu-Al LDH	375	416	6
PS/OCu-Fe LDH	357	415	5
PS/OCu-Cr LDH	385	423	13

TABLE IV
Water Uptake of PS/OLDH Nanocomposite Samples

Name of the sample	Water uptake (wt %)
Pure PS	2.89
PS/OMg-Al LDH	2.41
PS/OCu-Fe LDH	0.60
PS/OCu-Al LDH	1.54
PS/ONi-Al LDH	0.95
PS/OCo-Al LDH	1.09
PS/OCu-Cr LDH	1.16

Water uptake

The prepared PS/organically modified LDH nanocomposite films are tested for water uptake capacity and the results are reported in Table IV. It is revealed that the water uptake capacity of the nanocomposites is decreased in comparison to pristine polystyrene. The water uptake of pure PS film is found to be 2.89%, while the water uptake for PS/OCu-Fe LDH nanocomposite becomes 0.6%. The hydrophiliicity of LDHs is drastically reduced due to its treatment with SDS, which has displaced the outer and inner hydration shells that are coordinated to the inorganic cations.[35] In addition, the exfoliated LDH platelets present in the polystyrene matrix act as barrier and increase the mean effective path for the water molecules to travel, and also lead to an increase in water absorption resistance. From these data, we can conclude that the water uptake is negligible in case of PS/OLDH nanocomposites. Hence these nanocomposites are very much useful in preparing water proof ink and paint industry.

Acid and alkali stability test

Three samples of each nanocomposite films (having dimensions 3 cm $\times$ 3 cm) were dried at 100°C for 4 h to bring each sample to an identical starting state. The nanocomposite samples were then weighed to note the dry weight. Finally, the dried samples were individually soaked in 1*M* NaOH and 1*M* H_2SO_4 for 48 h. After that, the samples were taken out from acid and alkali solution and wiped with tissue paper. Then these samples were again dried in the oven at 100°C for 4 h and their dry weight was noted. No weight change was observed in case of all nanocomposite samples, which confirms that the synthesized PS nanocomposites are acid and alkali resistant. However, the color change is observed in case of PS/OCu-Fe LDH and PS/OCu-Cr LDH nanocomposites.

CONCLUSIONS

A series of PS/OLDH nanocomposites have been successfully developed by solvent blending method. The nano-dispersion of LDHs in the PS matrix for exfoliated structure has been verified by the disappearance of d_{003} (XRD) peak of LDHs. The thermal decomposition temperature of PS/OLDH nanocomposites is increased around 5–13°C indicating higher thermal stability compared to that of pure PS. The water uptake of the nanocomposites is negligible when compared with pure PS. The synthesized nanocomposites are stable in alkali and acid environment.

Authors are thankful to Centre for Nanotechnology, Central Instrument Facilities, and Department of Chemistry, IIT Guwahati for helping to carry out the XRD, TEM, SEM, and FTIR analysis, respectively.

References

1. Giannelis, E. P. Adv Mater 1996, 8, 29.
2. Usuki, A.; Kojima, Y.; Kawasumi, M.; Okada, A.; Fu-Jushima, A.; Kurauchi, T.; Kamigaito, O. J Mater Res 1993, 8, 1179.
3. Kojima, Y.; Usuki, A.; Kawasumi, M.; Okada, A.; Fu-Jushima, A.; Kurauchi, T.; Kamigaito, O. J Mater Res 1993, 8, 1185.
4. Lan, T.; Pinnavaia, T. J Chem Mater 1994, 6, 2216.
5. Messersmith, P. B.; Giannelis, E. P. Chem Mater 1994, 6, 1719.
6. Kojima, Y.; Fujushima, A.; Usuki, A.; Okada, A.; Kurauchi, T. J Mater Sci Lett 1993, 12, 889.
7. Gilman, J. W.; Kashiwagi, T. SAMPE J 1997, 33, 42.
8. Vaia, R. A.; Giannelis, E. P. MRS Bull 2001, 26, 394.
9. Gilman, J. W.; Jackson, C. L.; Morgan, A. B.; Harris, R.; Manias, E.; Giannelis, E. P.; Wuthenow, M.; Hilton, D.; Phillips, S. H. Chem Mater 2000, 12, 1866.
10. Gilman, J. W. Appl Clay Sci 1999, 15, 31.
11. Gilman, J. W.; Kashiwagi, T.; Morgan, A. B.; Harris, R. H.; Brassell, L. M.; VanLandingham, C. L.; Jackson, C. L. US Dept. Commerce, Technology Administration, National Institute of Standards and Technology, Report NISTIR #6531, Gaithersburg, VA, 2000.
12. Vaia, R. A.; Jandt, K. D.; Kramer, E. J.; Giannelis, E. P. Chem Mater 1996, 8, 2628.
13. Fornes, T. D.; Yoon, P. J.; Hunter, D. L.; Keskkula, H.; Paul, D. R. Polymer 2002, 43, 5915.
14. Yoon, P. J.; Hunter, D. L.; Paul, D. R. Polymer 2003, 44, 5323.
15. Dennis, H. R.; Hunter, D. L.; Chang, D.; Kim, S.; White, J. L.; Cho, J. W.; Paul, D. R. Polymer 2001, 42, 9513.
16. Zhu, J.; Morgan, A. B.; Lamelas, F. J.; Wilkie, C. A. Chem Mater 2001, 13, 3774.
17. Fan, X.; Zhou, Q.; Xia, C.; Cristofoli, W.; Mays, J.; Advincula, R. Langmuir 2002, 18, 4511.
18. Zhou, Q.; Fan, X.; Xia, C.; Mays, J.; Advincula, R. Chem Mater 2001, 13, 2465.
19. Velten, U.; Shelden, R. A.; Caseri, W. R.; Suter, U. W.; Li, Y. Macromolecules 1999, 32, 3590.
20. Meier, L. P.; Shelden, R. A.; Caseri, W. R.; Suter, U. W. Macromolecules 1994, 27, 1637.
21. Fu, X.; Qutubuddin, S. Polymer 2001, 42, 807.
22. Kim, Y. K.; Choi, Y. S.; Wang, M. H.; Chung, I. J Chem Mater 2002, 14, 4990.
23. Kim, T. H.; Jang, L. W.; Lee, D. C.; Choi, H. J.; Jhon, M. S. Macromol Rapid Commun 2002, 23, 191.
24. Park, C. I.; Park, O. O.; Lim, J. G.; Kim, H. Y. Polymer 2001, 42, 7465.
25. Kim, T. H.; Lim, S. T.; Lee, C. H.; Choi, H. J.; Jhon, M. S. J Appl Polym Sci 2003, 87, 2106.
26. Ma, J.; Xu, J.; Ren, J. H.; Yu, Z. Z.; Mai, Y. W. Polymer 2003, 44, 4619.
27. Morgan, A. B.; Gilman, J. W.; Jackson, C. L. Macromolecules 2001, 34, 2735.
28. Strawhecker, K. E.; Manias, E. Chem Mater 2000, 12, 2943.

29. Friedlander, H. Z.; Grink, C. R. J Polym Sci Polym Lett 1964, 2, 475.
30. Blumstein, A. J Polym Sci A 1965, 3, 2653.
31. Kato, C.; Kuroda, K.; Takahara, H. Clay Clay Miner 1981, 29, 294.
32. Kelly, P.; Moet, A.; Qutubuddin, S. J Mater Sci 1994, 29, 2274.
33. Akelah, A.; Kelly, P.; Qutubuddin, S.; Moet, A. Clay Miner 1994, 29, 169.
34. Akelah, A.; Moet, A. J Mater Sci 1996, 31, 3189.
35. Akelah, A.; Moet, A. Mater Lett 1993, 18, 97.
36. Vaia, R.; Ishii, H.; Giannelis, E. Chem Mater 1993, 5, 1694.
37. Doh, J. G.; Cho, I. Polym Bull 1998, 41, 511.
38. Sohn, J. I.; Lee, C. H.; Lim, S. T.; Kim, T. H.; Choi, H. J.; John, M. S. J Mater Sci 2003, 38, 1849.
39. Fu, X.; Tajuddin, Y.; Qutubuddin, S. AIChE Annu Meeting, Miami, FL, November 1998.
40. Uthirakumar, P.; Song, M. K.; Changwoon, N.; Lee, Y. S. Eur Polym J 2005, 41, 211.
41. Zhang, J.; Jiang, D. D.; Wang, D.; Wilkie, C. A. Polym Degrad Stabil 2006, 91, 2665.
42. Bhiwankar, N. N.; Weiss, R. A. Polym 2006, 47, 6684.
43. O'Leary, S.; O'Hare, D.; Seeley, G. Chem Commun 2002, 1506.
44. Leroux, F.; Basse, J. P. Chem Mater 2001, 13, 3507.
45. You, Y. W.; Zhao, H. T.; Vance, G. F. J Mater Chem 2002, 12, 907.
46. Newman, S. P.; Jones, W. N J Chem 1998, 22, 105.
47. Bhattacharjee, S.; Anderson, J. A. Chem Commun 2004, 554.
48. Ogwa, M.; Kuroda, K. Chem Rev 1995, 95, 399.
49. Takagi, K.; Shichi, T.; Usami, H.; Sawaki, Y. J Am Chem Soc 1993, 115, 4339.
50. Sels, B.; Vos, D. D.; Buntinx, M.; Pierard, F.; Mesmaeker, A. K.; Jacobs, P. Nature 1999, 400, 855.
51. Fogg, A. M.; Green, V. M.; Harvey, H. G.; O'Hare, D. Adv Mater 1999, 11, 1466.
52. Choy, J. H.; Kwak, S. Y.; Jeong, Y. J.; Park, J. S. Angew Chem Int Ed 2000, 39, 4042.
53. Vaysse, C.; Guerlou-Demourgues, L.; Duguet, E.; Delmas, C. Inorg Chem 2003, 42, 4559.
54. Whilton, N. T.; Vickers, P. J.; Mann, S. J Mater Chem 1997, 7, 1623.
55. Moujahid, E. M.; Besse, J. P.; Leroux, F. J Mater Chem 2003, 13, 258.
56. Oriakhi, C. O.; Farr, I. V.; Lerner, M. M. J Mater Chem 1996, 6, 103.
57. Yang, Q. Z.; Sun, D. J.; Zhang, C. G.; Wang, X. J.; Zhao, W. A. Langmuir 2003, 19, 5570.
58. Messersmith, P. B.; Stupp, S. I. J Mater Res 1992, 7, 2599.
59. Messersmith, P. B.; Stupp, S. I. Chem Mater 1995, 7, 454.
60. Challier, T.; Slade, R. C. T. J Mater Chem 1994, 4, 367.
61. Hsueh, H. B.; Chen, C. Y. Polymer 2003, 44, 1151.
62. Hsueh, H. B.; Chen, C. Y. Polymer 2003, 44, 5275.
63. Chen, W.; Qu, B. J Chem Mater 2003, 15, 3208.
64. Chen, W.; Feng, L.; Qu, B. J Chem Mater 2004, 16, 368.
65. Qiu, L.; Qu, B. J Coll Interf Sci 2006, 301, 347.
66. Tao, Q.; Zhang, Y.; Zhang, X.; Yuan, P.; He, H. J Solid State Chem 2006, 179, 708.
67. Qiu, L.; Chen, W.; Qu, B. Polym Degrad Stabil 2005, 87, 433.
68. Ding, P.; Qu, B. J Coll Interf Sci 2005, 291, 13.
69. Du, L.; Qu, B.; Meng, Y.; Zhu, Q. Compos Sci Technol 2008, 66, 913.
70. Carpentiera, F.; Bourbigot, S.; Le Bras, M.; Delobelb, R.; Foulon, M. Polym Degrad Stabil 2000, 69, 83.